0013-4651/2011/158(10)/H983/5/$28.00 © The Electrochemical Society

Improvement of (11-22) GaN on m-Plane Sapphire With CrN Interlayer by Using Molecular Beam Epitaxy

Kuang-Wei Liu,[a] Shoou-Jinn Chang,[a,c,z] Sheng-Joue Young,[b,z] Tao-Hung Hsueh,[a] Hung Hung,[c] Yu-Chun Mai,[a] Shih-Ming Wang,[c] and Yue-Zhang Chen[d]

[a]*Institute of Electro-Optical Science and Engineering,* [c]*Institute of Microelectronics and Department of Electrical Engineering, and* [d]*Institute of Nanotechnology and Microsystems Engineering, National Cheng Kung University, Tainan 701, Taiwan*
[b]*Department of Electronic Engineering, National Formosa University, Yunlin 632, Taiwan*

This study investigates the crystalline quality, surface, and optical properties of semi-polar GaN (11 $\bar{2}$ 2) grown on m-sapphire substrates with and without a CrN interlayer using molecular beam epitaxy (MBE). The results of the characterization performed by an X-ray diffraction system, scanning electron microscopy and photoluminescence system, all indicate that the crystalline quality, threading dislocation, surface morphology and optical properties of (11$\bar{2}$2) GaN grown with the CrN were superior to those when CrN was not inserted. Details of defect-related emissions of these two samples were observed and investigated in temperature dependent PL measurements, with a low temperature PL spectrum. A weak basal stacking fault related (BSF-related) emission at 3.432 eV was observed in these two samples. In comparison, the BSF-related emission peak as a shoulder to the near band edge (NBE) peaks for the semi-polar GaN grown without CrN was hardly distinguishable at a low temperature.
© 2011 The Electrochemical Society. [DOI: 10.1149/1.3615957] All rights reserved.

Manuscript submitted March 15, 2011; revised manuscript received June 1, 2011. Published August 2, 2011.

Group III-V related nitride semiconductors and their alloys containing Ga, In and Al have great potential for application in visible and ultraviolet optoelectronic, and high-temperature and high power electronic devices due to their wide band-gaps and good thermal stability.[1] In particular, GaN has the advantages of a wide band-gap (3.4 eV), and excellent chemical and thermal stability. Epitaxial film quality is of great importance to the success of all nitride-base optoelectronic devices. However, a large lattice mismatch between the GaN and sapphire leads to cracks or dislocations in the GaN films.[2] Moreover, the induced strain leads to a piezoelectric effect that reduces the recombination efficiency because the polarization discontinuities cause band bending due to the quantum confined Stark effect (QCSE).[3] Recently, non-polar GaN of *m*-plane orientation has offered the potential of improved efficiency[4,5] compared to devices fabricated with the conventional *c*-plane GaN orientation. Therefore, nonpolar and semipolar GaN grown on $LiAlO_2$ (100) (Ref. 6) and SiC (1$\bar{1}$00) (Ref. 7) substrates have been investigated. However, none of these substrates possesses all the advantages of sapphire, which include chemical stability, optical transparent and low cost. GaN grown on the *m*-plane sapphire provided an alternative choice to semi-polar GaN. For example, Baker et al. demonstrated that the orientation of GaN grown on *m*-plane sapphire was along the (10$\bar{1}$3) or (11$\bar{2}$2) direction,[8] and electroluminescence from semi-polar InGaN/GaN light emitting diodes has shown a reduced blue-shift with a rising drive current compared to the light emitting diodes grown on the c-plane sapphire, indicating a reduced polarization in the active layer.[9] However, the (11$\bar{2}$2) plane was observed as the sidewall plane for V-defects in GaN grown by the MBE system,[10] and these studies demonstrated that nonpolar and semipolar GaN effectively decreased the piezoelectric effect, and the efficiency was clearly improved. Considering the high cost of the $LiAlO_2$ and SiC substrates, the m-plane sapphire is better choice as substrates. On the other hand, the surface morphology caused by these V-defects resulted in a rough surface of the m-plane sapphire is still to be improved, to improve the rough surface and crystalline quality of GaN grown on m-plane sapphire, *X. Ni* et al. reported that the quality of semi-polar GaN (11$\bar{2}$2) grown on m-plane sapphire could be improved by epitaxy lateral overgrowth (ELO).[11] Recently, high quality c-axis GaN epitaxial layers have grown by using CrN buffer layer, which is due to the lattice constant of the cubic CrN is between sapphire and GaN,[12] For this reason, we expect the crystalline quality of the semi-polar GaN grown on CrN/m-plane sapphire could be increased by inserting the CrN interlayer. In this study, we used CrN as an interlayer between the low temperature GaN (LT-GaN) and the GaN epilayer. Furthermore, the effect of CrN inserted was investigated by characterizing the growth orientation and optical properties.

[z] E-mail: changsj@mail.ncku.edu.tw; shengjoueyoung@gmail.com

Experiment

In this study, GaN was deposited on *m*-sapphire (10$\bar{1}$0) substrates in a MBE system (SVT ASSOCIATES, INC.) with a radio frequency (RF) nitrogen plasma source. A discharge power of 350 W and a gas flow rate of 1.2 sccm were used to generate N_2 plasma at a background pressure of 1.8×10^{-9} Torr. The *m*-sapphire substrates were initially cleaned, dipped in a 20% HCl solution, rinsed in de-ionized water, dried in an oven, and placed immediately into the vacuum chamber of the MBE system to grow a low temperature GaN (LT-GaN) nucleation layer 30 nm thick. The growth rate was estimated to have been around 1 nm/min. To form the CrN interlayer, the Cr metal was deposited on the LT-GaN nucleation layers by RF-sputter. The samples were then nitrided in an MBE chamber prior to the growth of the GaN epilayer. Because the nitridation process can occur on the surface with a depth of several nanometers, a 20 nm Cr thin film was deposited on the LT-GaN/m-plane sapphire template in this study. The Cr-coated LT-GaN template was then treated with N_2 plasma at a substrate temperature of 700°C for 30 min in the MBE system. Following the step, the GaN epilayer layer was grown under gallium-rich conditions directly on top of the nitridated Cr-coated substrate at a temperature of 750°C. The main GaN epilayers were then grown at a substrate temperature of 750°C for 2 h. The growth rate of the GaN epilayer was typically around 300 nm/h in this study. The surface changes of all samples were monitored by *in situ* RHEED during growth along the [11$\bar{2}$2] azimuth. For comparison, a GaN epilayer grown on an m-sapphire substrate without CrN interlayers was also prepared. The crystallographic orientation and crystalline quality were examined with X-ray diffraction (XRD), and an X-ray diffraction rocking curve (XRC), and the surface morphology was examined by scanning electron microscope (SEM). The emission properties of semi-polar GaN(11$\bar{2}$2) grown on m-plane sapphire were investigated by temperature dependent photoluminescence (PL) measurements, and the photoluminescence system included a 30 mW He-Cd laser with a wavelength of 365 nm.

Results and Discussion

To determine the crystallographic orientation and crystalline quality, the as-grown GaN films on *m*-plane sapphire were examined

Downloaded 16 Sep 2011 to 141.213.172.42. Redistribution subject to ECS license or copyright; see http://www.ecsdl.org/terms_use.jsp

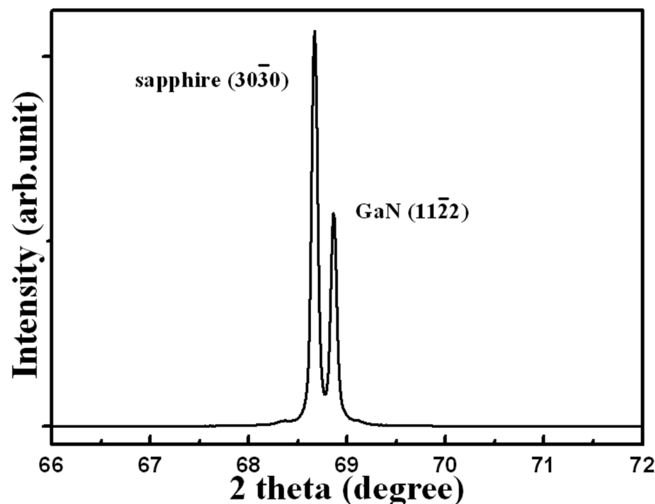

Figure 1. XRD-2θ scan for GaN grown on m-plane sapphire, this result indicated the surface orientation of GaN was $(11\bar{2}2)_{GaN}||(10\bar{1}0)_{sapphire}$.

by a high-resolution XRD system. Figure 1 shows the XRD 2θ scan spectra of GaN grown on m-plane sapphire without a CrN interlayer, the locations of the XRD spectra peaks of the sample with the CrN interlayer are similar to those samples without a CrN interlayer, as shown in Fig. 1. The main XRD peaks are 68.67 and 68.92°, which corresponded to sapphire (30$\bar{3}$0) and GaN (11$\bar{2}$2), respectively.[8] It should be noted that the surface orientation relationship of GaN was $(11\bar{2}2)_{GaN}||(10\bar{1}0)_{sapphire}$, which corresponded with Ref. 11. However, because the resolution was too low to identifiy the crystalline quality of these two samples by an XRD 2θ scan, the peaks of GaN (11$\bar{2}$2) were examined by a high resolution double crystal XRD system. Figure 2a shows the results of the high resolution ω-2θ scan of GaN (11$\bar{2}$2) reflection. The FWHM of the sample with and without the CrN inserting layer were 332 and 670 arcsec, respectively. The improvement of the semi-polar GaN crystalline quality and the reduction of the stacking fault may result from the stress relaxation by inserting the CrN layer,[13,14] because the CrN has a lattice constant between GaN and sapphire. However, ω-2θ is not typically determined by the bowing of the thick films due to residual stress, so a symmetric X-ray rocking curve was employed to confirm the threading dislocation. Figures 2b and 2c show the results of the on-axis (11$\bar{2}$2) rocking direction along the sapphire *c-axis* (0001) and the *a-axis* (1$\bar{2}$10) reflections, respectively. While semi-polar GaN grown with an inserted CrN layer shows lower FWHMs of only 1614 and 2058 arcsec measured in the corresponding direction, the FWHM values of semi-polar GaN grown without inserting a CrN layer are 3616 and 2628 arcsec, respectively. It is reasonable to speculate the threading dislocation and residual stress of semi-polar GaN may be reduced by inserting the CrN layer,[13,14] regardless of the dislocations is along the $(0001)_{sapphire}$ or the $(10\bar{1}0)_{sapphire}$ direction. The reason why the dislocation is reduced is that CrN can effectively mask the propagation of the dislocations by bending the dislocation directions. For the epilayer grown with an inserted layer of CrN, the comparatively narrow distribution of crystalline tilt indicated that a relatively high level of crystalline quality from the FWHM shows less anisotropy in the in-axis mosaic with the inserted CrN. This anisotropic behavior is caused by the anisotropic growth, and is mostly related to the distribution of unavoidable defects. The isotropic structure can be expected to exhibit nonpolar or semi-polar growth with the crystalline quality improved by the inserted CrN.

Because the XRD and XRC system cannot identify the surface morphology, SEM was employed to inspect the surface of these two samples, and the morphology plan-views of the samples with and without CrN are shown in Figs. 3a and 3b, respectively.

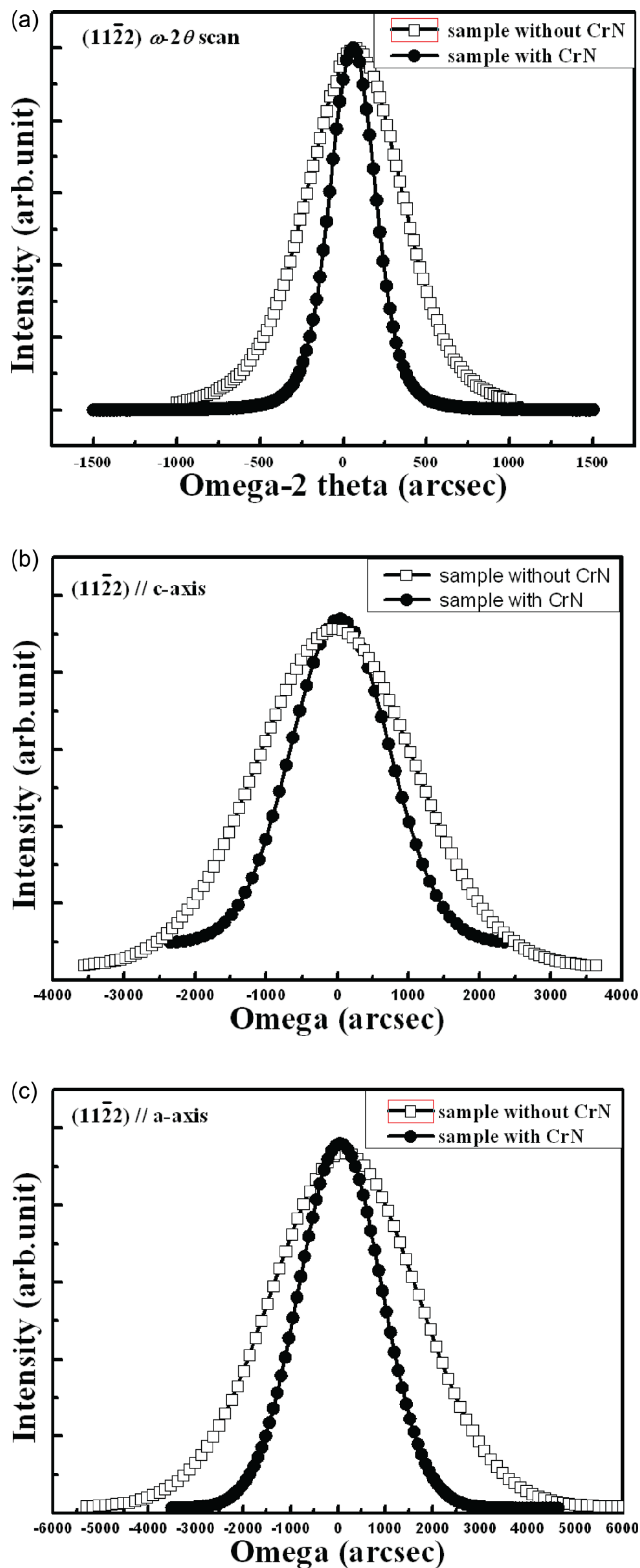

Figure 2. (Color online) (a) ω-2θ scan (b) ω scan//c-axis (c) ω scan//a-axis of symmetrical GaN (11$\bar{2}$2) grown with and without CrN inserted CrN.

Figure 3a is indicative of a rough morphology with V-shaped features that are oriented along the *c-axis* direction of the sapphire, and threading dislocation pits located at the corners of V-shaped features.[11] It is worth noting that these V-shaped features not only

Downloaded 16 Sep 2011 to 141.213.172.42. Redistribution subject to ECS license or copyright; see http://www.ecsdl.org/terms_use.jsp

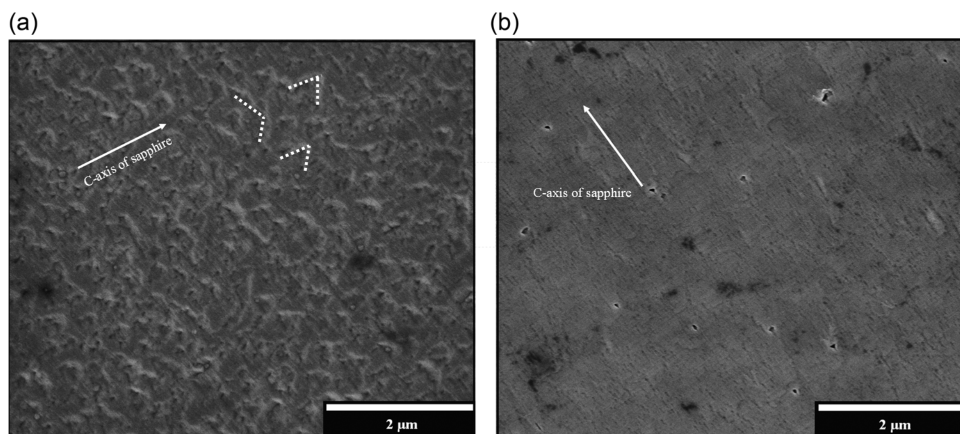

Figure 3. SEM images of semi-polar GaN (11$\bar{2}$2) (a) without CrN inserted ("V-shape defects" has been marked by dashed line) (b) with CrN inserted.

provide a morphological anisotropy, but may also reflect the density of the basal-plane stacking faults. In contrast, as showed in Fig. 3b, a similar result to previous nonpolar GaN thin films[15] and slate-like patterns is clearly observed on the surface of the sample with the inserted CrN. The striated direction was parallel to the *c-axis* direction, and the V-shaped features were replaced by a slate-like pattern, meaning that the basal-plane stacking faults decreased when the CrN was inserted. It also implies that the insertion of CrN can improve the surface roughness. Using atomic force microscope (AFM), the surface root-mean-square (RMS) roughnesses of non-polar GaN with and without the inserted CrN were 4.8 nm and 8.5 nm, respectively.

Further evidence of the improvement in the crystallinity by inserting CrN was measured using photoluminescence (PL) at 20 K. Figure 4 shows the low-temperature PL spectra of semi-polar GaN with and without inserting the layer of CrN. The spectra of GaN (11$\bar{2}$2) film without the inserted CrN showed three main emission bands located at 3.472, 3.432 and 3.291 eV. The 3.472 eV emission band, according to previous results of non-polar GaN, may correspond with the common GaN near bandedge emission (NBE).[16] The 3.432 emission band was attributed to a type I_1 basal-plane stacking fault (BSF), and the 3.291 eV emission band was due to impurities in the partial dislocation, and the mechanism of emission was due to donor-acceptor pair (DAP) emission.[17] Compared to GaN grown without the inserted CrN, a slight red-shift around 2 meV in the NBE peak energy with the inserted CrN was observed. This red-

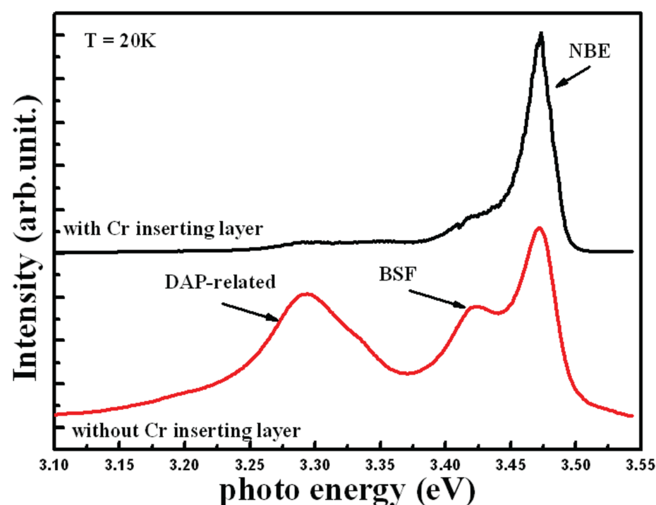

Figure 4. (Color online) Low temperature PL spectra of (11$\bar{2}$2) GaN grown on m-sapphire with and without CrN.

shift of the NBE in the GaN grown with the inserted CrN may be attributed to the partial relief of the compressive stress during the growth process. Notably, the BSF-related peaks from the GaN with and without the inserted CrN were located at 3.432 and 3.438 eV, respectively, and exhibited a blue-shift of around 6 meV. A similar result has been reported in Ref. 19, which found that BSF-related emissions may arise from bundles of BSF. However, considering the different spatial distribution of BSF, the blue-shift does not reflect the strain variation.

The PL results also corroborated the XRC result for GaN grown with and without the inserted CrN; the FWHM of the NBE peaks of GaN grown with and without the inserted CrN is 22.4 and 27.78 meV, respectively. This narrow emission indicated that the crystalline quality of semi-polar GaN was improved by inserting CrN. For the GaN grown without the inserted CrN, the intensity of BSF emission is similar to NBE emission. On the contrary, the BSF emission appears as a shoulder of the NBE peak, and the relative intensity between BSF and NBE emissions in the GaN grown with the inserted CrN had greatly decreased, this behavior indicated that the crystallographic defect density had reduced. We speculate that the different lattice structure of the CrN nanoislands reduce the compressive stress, lead to the formation of BSF may be inhibited.

To investigate the optical properties of semi-polar GaN (11$\bar{2}$2), we performed a detailed study of these two samples with temperature dependent PL ranging from 20 to 300 K. For clarity, the temperature dependence of the observed PL signal, and the normalized PL intensity of GaN with and without the inserted CrN are shown in Figs. 5a and 5b. These two spectra clearly show that there was an apparent decrease in intensity and red shift for the NBE as the temperature increased, and both spectra of these two samples were similar at room temperature. However, the PL intensity of semi-polar GaN grown with inserted CrN was ten times larger than GaN grown without the inserted CrN at room temperatures, which probably originated from the ameliorated crystalline quality of GaN, owing to the rough surface of deteriorated crystalline quality scattered part of PL signal. In Fig. 5b, the BSF-related emission decreased faster than NBE as the temperature increased. This result was in agreement with the previous study in *a*-plane GaN.[18] On the other hand, the BSF related emission turned into a shoulder above 40 K and disappearing above a temperature of approximately 120 K. Nevertheless, the NBE peak remained up to room temperature and dominated the PL spectra. A similar behavior occurred in GaN grown with the inserted CrN. In Fig. 5a, the difference was that the NBE peak dominated the PL spectra at 20 K. T. B. Wei et al. found that the BSF-related emission was due to the peak that arises from the recombination of exictions bound to I_1-BSF at a lower temperature, and that the peak was due to the thermally induced electrons delocalized from the BSF at a higher temperature.[19] In contrast, the BSF-related emission in the PL spectra of

Downloaded 16 Sep 2011 to 141.213.172.42. Redistribution subject to ECS license or copyright; see http://www.ecsdl.org/terms_use.jsp

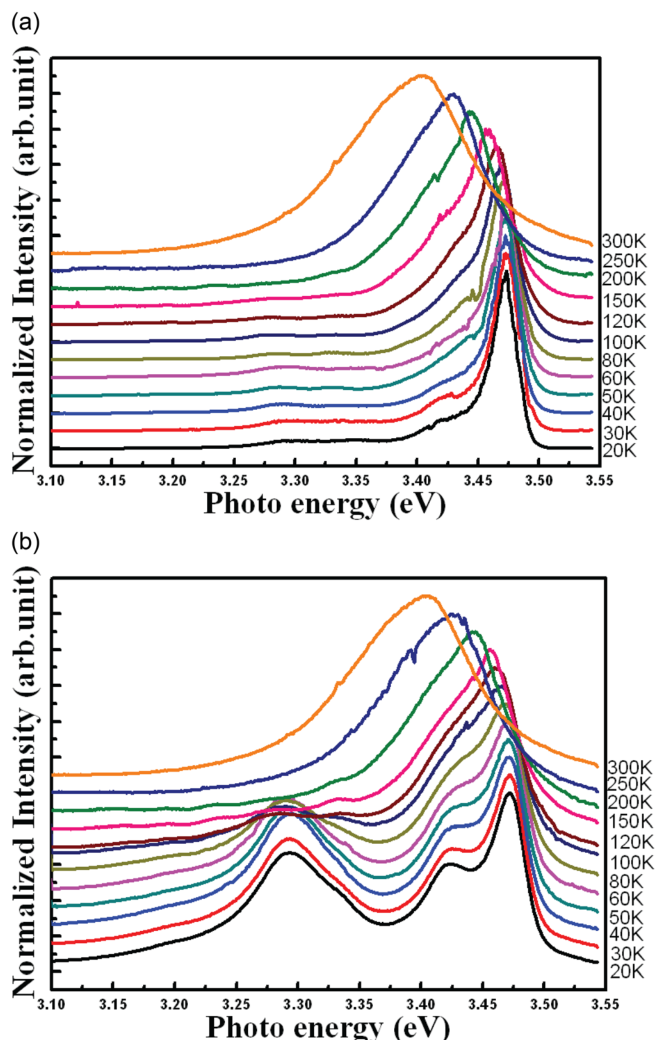

Figure 5. (Color online) Temperature dependent PL spectra of $(11\bar{2}2)$ GaN (a) with CrN inserted (b) without CrN inserted.

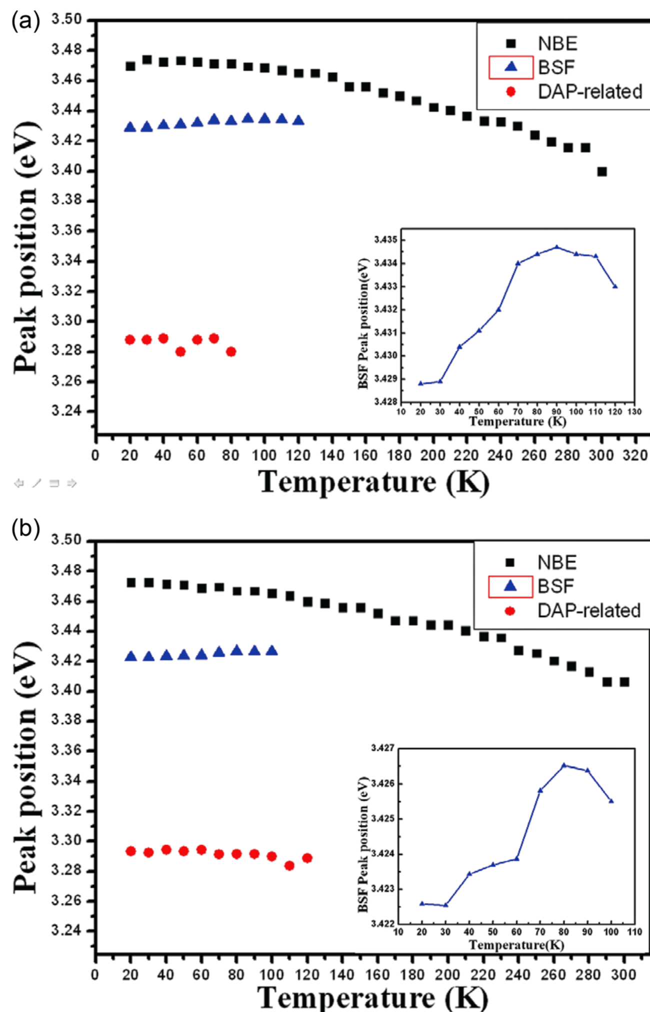

Figure 6. (Color online) Peak energy position of NBE, DAP-related emission and DAP-related emission from the $(11\bar{2}2)$ GaN grown (a) with CrN inserted (b) without CrN inserted.

the semi-polar GaN grown with the inserted CrN was relatively lower and the NBE peak at the lower temperature was due to the BSF reduced by the improved crystalline quality.

Finally, the temperature dependence of the peak energy position of the NBE, BSF-related emission and DAP-related emission of semi-polar GaN grown with and without the inserted CrN are shown in Figs. 6a and 6b. The NBE peak follows Varshni's formula, $E_g(T) = E_g(0) - \alpha T^2/(\beta + T)$, where $E_g(T)$ is the corresponding energy at 0 K, and α and β are known as the Varshini's formula thermal coefficient and the Debye temperature. The best fit was obtained with $\alpha = 6.7 \times 10^{-4}$ and 6.7×10^{-4} eV/K and $\beta = 820$ and 930 K for semi-polar GaN grown with and without the inserted CrN, respectively. Both of these values were within the range reported by the previous study.[18–20] In Fig. 6a, it is worth noting that the position of the BSF-related emission has typical S-shaped of temperature dependence, this S-shaped behavior indicates that the 3.432 eV emissions arise from localized excitons, these excitons are bound in the stacking fault.[19] On the other hand, the DAP-related peak at 3.291 eV is rapidly quenched and it is difficult to identify at 60 and 120 K for semi-polar GaN grown with and without the inserted CrN, respectively. T. B. Wei et al. speculated that the holes delocalize from the BSF which are re-captured by defects,[20] may be threading dislocations, Ga-vacancies or N-vacancies in low quality GaN. In addition, because of the defects reduced by CrN being inserted, DAP-related emissions only persists up to 60 K.

Conclusion

In conclusion, we have demonstrated the growth of semi-polar GaN $(11\bar{2}2)$ on an m-plane sapphire substrate with a CrN interlayer. The influence of the inserted CrN on the crystalline quality and the dislocations has been demonstrated by an HR-XRD system. The results of the ω-2θ scan indicate that the stacking fault was inhibited by the inserted CrN. The results of the XRC ω-scan indicate that threading dislocations were suppressed due to the different lattice structures of CrN tending to block the threading dislocations. Further evidence of an improvement in crystalline quality was provided by the surface morphology of the SEM images. The V-shaped defects on the semi-polar GaN were eliminated due to the stacking faults being reduced. Because of the temperature dependent PL measurements, three emission mechanisms, NBE (3.472 eV), BSF-related (3.432 eV) and DAP-related (3.291 eV), were observed in low temperature and temperature dependent PL measurements of semi-polar GaN grown with and without the CrN interlayer. PL measurements provided further evidence of crystalline quality improvement with the inserted CrN.

Acknowledgment

This work was supported by National Science Council of Taiwan under Contract Nos. NSC 100-2221-E-150-057, NSC 99-2218-E-150-003

Downloaded 16 Sep 2011 to 141.213.172.42. Redistribution subject to ECS license or copyright; see http://www.ecsdl.org/terms_use.jsp

and NSC 99-2622-E-150-012-CC3. National Formosa University Research and Services Headquarters that provided the partial equipment for measurement is also acknowledged.

This work was also supported in part by the Center for Frontier Materials and Micro/Nano Science and Technology, National Cheng Kung University (NCKU), Taiwan (D97-2700), and in part by the Advanced Optoelectronic Technology Center, NCKU, under projects from the Ministry of Education.

References

1. L. F Eastman and U.K. Mishra, *IEEE Spectrum*, **39**, 28 (2002).
2. E. Feltin, B. Beaumont, M. Laügt, P. de Mierry, P. Vennèguès, H. Lahrèche, M. Leroux, and P. Gibart, *Appl. Phys. Lett.*, **79**, 3230 (2001).
3. F. Bernardini, V. Fiorentini, and D. Vanderbilt, *Phys. Rev. B*, **56**, R10024 (1997).
4. K. Okamoto, H. Ohta, S. F. Chichibu, J. Ichihara, and H. takasu, *Jpn. J. Appl. Phys.*, Part 2, **46**, L187 (2007).
5. M. C. Schmidt, K.-C. Kim, H. Sato, N. Fellows, H. Masui, S. Nakamura, S. P. DenBaars, and J. S. Speck, *Jpn. J. Appl. Phys.*, Part 2, **46**, L126 (2007).
6. P. Waltereit, O. Brandt, A. Trampert, H. T. Grahn, J. Menniger, M. Ramsteiner, M. Reiche, and K. H. Ploog, *Nature*, **406**, 865 (2000).
7. N. F. Gardner, J. C. Kim, J. J. Wierer, Y. C. Shen, and M. R. Krames, *Appl. Phys. Lett.*, **86**, 111101 (2005).
8. T. J. Baker, B. A. Haskell, F. Wu, J. S. Speck, and S. Nakamura, *Jpn. J. Appl. Phys.*, **45**(6), L154 (2006).
9. R. Sharma, P. M. Pattison, H. Masui, R. M. Farrell, T. J. Baker, B. A. Haskell, F. Wu, S. P. DenBaars, and J. S. Speck, *J. Appl. Phys.*, **94**, 942 (2003).
10. B. Heying, R. Averbeck, L. F. Chen, E. Haus, H. Riechert, and J. S. Speck, *J.Appl. Phys.*, **88**, 1855 (2000).
11. X. Ni, Ü. Özgür, A. A. Baski, and H. Morkoc, *Appl. Phys. Lett.*, **90**, 182109 (2007).
12. W. H. Lee, S. W. Lee, H. Goto, H. C. Ko, M. W. Cho, and T. Yao, *Phys. Status. Solidi C*, **3**(6), 1388 (2006).
13. W. Lee, S. Lee, H. Goto, H. Ko, M. Cho, and T. Yao, *Phys. Status Solidi C*, **3**(6), 1388 (2006).
14. J. S. Ha, H. J. Lee, S. W. Lee, H. J. Lee, S. H. Lee, H. Goto, M. W. Cho, T. Yao, S. K. Hong, R. Toba, et al., *Appl. Phys. Lett.*, **92**, 091906 (2008).
15. R. Armitage, M. Horita, J. Suda, and T. Kimito, *J. Appl. Phys.*, **101**, 033534 (2007).
16. R. Liu, A. Bell, F. A. Ponce, C. Q. Chen, J. W. Yang, and M. A. Khan, *Appl. Phys. Lett.*, **86**, 021908 (2005).
17. T. Guhne, Z. Bougrioua, S. Laugt, M. Nemoz, P. Vennegues, B. Vinter, and M. Leroux, *Phys. Rev. B*, **77**, 075308 (2008).
18. P. P. Paskov, R. Schifano, B. Monemar, T. Paskov, S. Figge, and D. Hommel, *J. Appl. Phys.*, **98**, 093519 (2005).
19. T. B. Wei, Q. Hu, R. F. Duan, X. C. Wei, J. K. Yang, J. X. Wang, Y. P. Zeng, G. H. Wang, and J. M. Li, *J. Electrochem. Soc.*, **157**, H721 (2010).
20. R. Pässler, *J. Appl. Phys.*, **90**, 3956 (2001).

Downloaded 16 Sep 2011 to 141.213.172.42. Redistribution subject to ECS license or copyright; see http://www.ecsdl.org/terms_use.jsp